Functional Characterization of the Arabidopsis AtSUC2 Sucrose/H^+ Symporter by Tissue-Specific Complementation Reveals an Essential Role in Phloem Loading But Not in Long-Distance Transport[1][OA]

Avinash C. Srivastava[2], Savita Ganesan[3], Ihab O. Ismail, and Brian G. Ayre*

Department of Biological Sciences, University of North Texas, Denton, Texas 76203–5220

AtSUC2 (At1g22710) encodes a phloem-localized sucrose (Suc)/H^+ symporter necessary for efficient Suc transport from source tissues to sink tissues in Arabidopsis (*Arabidopsis thaliana*). *AtSUC2* is highly expressed in the collection phloem of mature leaves, and its function in phloem loading is well established. *AtSUC2*, however, is also expressed strongly in the transport phloem, where its role is more ambiguous, and it has been implicated in mediating both efflux and retrieval to and from flanking tissues via the apoplast. To characterize the role of AtSUC2 in controlling carbon partitioning along the phloem path, *AtSUC2* cDNA was expressed from tissue-specific promoters in an *Atsuc2* mutant background. Suc transport in this mutant is highly compromised, as indicated by stunted growth and the accumulation of large quantities of sugar and starch in vegetative tissues. Expression of *AtSUC2* cDNA from the 2-kb *AtSUC2* promoter was sufficient to restore growth and carbon partitioning to nearly wild-type levels. The *GALACTINOL SYNTHASE* promoter of *Cucumis melo* (*CmGAS1p*) confers expression only in the minor veins of mature leaves, not in the transport phloem of larger leaf veins and stems. Mutant plants expressing *AtSUC2* cDNA from *CmGAS1p* had intermediate growth and accumulated sugar and starch, but otherwise they had normal morphology. These characteristics support a role for AtSUC2 in retrieval but not efflux along the transport phloem and show that the only vital function of AtSUC2 in photoassimilate distribution is phloem loading. In addition, *Atsuc2* mutant plants, although debilitated, do grow, and *AtSUC2*-independent modes of phloem transport are discussed, including an entirely symplastic pathway from mesophyll cells to sink tissues.

Transport of water and dissolved nutrients through the phloem is along hydrostatic pressure gradients: source-leaf phloem accumulates solute, and the influx of water by osmosis generates pressure. Metabolism in sink tissues lowers the solute concentration and causes water and pressure to dissipate. The open lumen of the sieve tubes permits bulk flow of sap from source to sink along the resulting pressure differential. Based on its role in nutrient distribution and its location in the plant, the phloem network is commonly divided into the collection phloem, the release phloem, and the transport phloem (van Bel, 1996). In source tissues, nutrients enter the phloem network via the collection phloem and are released in sink tissues from the release phloem. The transport phloem connects source and sink tissues and represents the longest contiguous stretch of phloem in the long-distance-transport pathway.

Transport events in the collection and release phloem have received the most scrutiny, whereas the transport phloem is underrepresented (Lalonde et al., 2003; van Bel, 2003). Most plants expend energy in the collection phloem to accumulate sugar and accentuate the pressure gradient between source and sink tissues (Turgeon and Ayre, 2005). This is called phloem loading, and in many systems, Suc is loaded from the apoplast into the collection phloem by Suc-proton (Suc/H^+) symporters (Giaquinta, 1977; Lalonde et al., 2003). In dicotyledonous plants, *SUT1* (*AtSUC2* in Arabidopsis [*Arabidopsis thaliana*]) is the predominant, and perhaps exclusive, Suc/H^+ symporter catalyzing this process. Nutrient unloading in the release phloem may occur through plasmodesmata (i.e. unloading through the symplast) or across membranes to the apoplast, followed by retrieval into recipient cells (Patrick, 1997; Lalonde et al., 2003). How Suc enters the apoplast in source tissues in preparation for loading and in sink tissues during unloading is not clear, since a clear efflux carrier has not emerged (Lalonde et al., 2003; van Bel, 2003; Sauer, 2007).

The transport phloem both unloads and retrieves photoassimilate in a process that nourishes flanking tissues and mobilizes sugars to and from short- and

[1] This work was supported by the National Science Foundation, Division of Integrative Organismal Systems (grant no. 0344088).

[2] Present address: Samuel Roberts Noble Foundation, Plant Biology Division, Ardmore, OK 73401.

[3] Present address: Amyris Biotechnologies, Inc., Emeryville, CA 94608.

* Corresponding author; e-mail bgayre@unt.edu.

The author responsible for distribution of materials integral to the findings presented in this article in accordance with the policy described in the Instructions for Authors (www.plantphysiol.org) is: Brian G. Ayre (bgayre@unt.edu).

[OA] Open Access articles can be viewed online without a subscription.

www.plantphysiol.org/cgi/doi/10.1104/pp.108.124776

long-term storage reserves (van Bel, 2003). In the stem of *Phaseolus vulgaris*, for example, Suc efflux from the transport phloem was 6% cm^{-1} and retrieval was 3% cm^{-1} (Minchin and Thorpe, 1987). Suc retrieval is mediated by Suc/H^+ symporters, as indicated by treating stems with *p*-chloromercuribenzenesulfonic acid, a reagent that modifies sulfhydryl groups and inhibits the transport of Suc across plasma membranes (Giaquinta, 1976; Aloni et al., 1986; Hayes et al., 1987; Minchin and Thorpe, 1987; Grimm et al., 1997), and based on expression pattern, retrieval in the transport phloem is most likely catalyzed by the same symporters that catalyze loading in the collection phloem (Truernit and Sauer, 1995; Kuhn et al., 2003). The mechanism for Suc efflux to the transport phloem apoplast is unclear, since, as described above for the collection and release phloem, a clear efflux carrier is not identified. Suc/H^+ symporters are implicated, however, as treating stems with *p*-chloromercuribenzenesulfonic acid is reported to inhibit both efflux and retrieval (Aloni et al., 1986; Hayes et al., 1987). In addition, Frommer and colleagues, based on immunolocalization and protein-protein interaction studies with potato (*Solanum tuberosum*) SUT proteins, speculated that Suc/H^+ symporters could form specific interactions with other cellular components to promote facilitated diffusion across the membrane (Reinders et al., 2002; Kuhn et al., 2003). It was also shown that *ZmSUT1* from maize (*Zea mays*) can operate in either direction, depending on the membrane potential, pH, and Suc concentrations across the membrane (Carpaneto et al., 2005).

Contradicting a potential role for Suc/H^+ symporters in efflux from the phloem is evidence for nonspecific, passive efflux of disaccharides and other small solutes to the apoplast. When galactinol, a nonreducing disaccharide composed of Gal and myoinositol, was synthesized in minor vein phloem, long-distance transport of galactinol was limited and substantial quantities were identified in the lamina and apoplast of mature leaves, because, it was speculated, galactinol leaked from the phloem during transport and was redistributed in the leaf by xylem transport (Ayre et al., 2003). Similarly, the Suc isomer palatinose, which is not recognized by Suc transporters, demonstrated nonspecific transport across membranes in transgenic tobacco (*Nicotiana tabacum*) expressing a Suc isomerase gene. Although the enzyme localized to the apoplasm, palatinose was identified in all cellular compartments, including the stroma of chloroplasts (Bornke et al., 2002).

To further assess the role of Suc/H^+ symporters in whole plant carbon partitioning, *AtSUC2* expression was confined to the collection phloem by expressing *AtSUC2* cDNA from the *Cucumis melo GALACTINOL SYNTHASE* gene promoter (*CmGAS1p*) in a homozygous *Atsuc2* mutant background. *CmGAS1p* is active only in the minor veins of mature leaves (i.e. collection phloem), such that mutant plants harboring this construct lack *AtSUC2* activity in the transport phloem. These plants were able to phloem load, but long-distance transport was not subject to further influence from *AtSUC2*. The *AtSUC2* promoter was used as a positive control for complementation studies, and transgenic plants were characterized for general growth, sugar distribution, and transport efficiency. The results support a role for AtSUC2 in retrieval, but not efflux, along the transport phloem, and they also show that the only "essential" role for AtSUC2 is loading in the collection phloem. Furthermore, growth of the *Atsuc2* mutant plants, although minimal, implies phloem transport, and this is discussed in relation to whether AtSUC2 and phloem loading are necessary for phloem transport in Arabidopsis.

RESULTS

Identifying *Atsuc2*::*T-DNA* Mutations

Three lines with T-DNA insertions at the *AtSUC2* locus (At1g22710) were obtained through the Arabidopsis Biological Resource Center: SALK_087046, SALK_001331, and SALK_038124 (Alonso et al., 2003). Twelve seedlings from each line were genotyped by PCR for *AtSUC2* disruption with a T-DNA-specific oligonucleotide and two oligonucleotides flanking the putative T-DNA insertion site. An insert was not identified among SALK_087046 seedlings sampled, and a single plant homozygous for an insert was identified among the SALK_001331 seedlings. The insert in SALK_001331 is located downstream of the *AtSUC2* open reading frame, and a phenotype was not observed. Several SALK_038124 seedlings were heterozygous *AtSUC2/Atsuc2*::*T-DNA* (designated *AtSUC2* +/−). Progeny of SALK_038124 segregating homozygous *Atsuc2*::*T-DNA*/*Atsuc2*::*T-DNA* (designated *AtSUC2* −/−) were severely stunted and accumulated anthocyanin and starch in mature leaves (Fig. 1A), as described previously for three other mutants with T-DNA insertions at the *AtSUC2* locus (Gottwald et al., 2000). One of these contained an insertion in the first intron, and the other two contained insertions in the second intron. All three had the same phenotype and were considered knockout mutations (Gottwald et al., 2000). The SALK_038124 T-DNA insertion site was sequenced and confirmed to be in the second intron, 1,473 nucleotides downstream of the start codon in the genomic sequence (Fig. 1B).

Total RNA was isolated from SALK_038124 plants segregating *AtSUC2* +/+, +/−, and −/− for semiquantitative transcript analysis relative to a ubiquitin gene, *UBQ10* (Weigel and Glazebrook, 2002). Oligonucleotides specific to a region upstream of the T-DNA insert showed that the 5′ region of the *AtSUC2* transcript is present in *AtSUC2* −/− plants, but at reduced levels relative to *AtSUC2* +/+ plants (Fig. 1C). These bands are not due to genomic DNA contamination, since the RNA was treated with DNase, and control samples without reverse transcriptase treatment did not produce PCR products. Oligonucleotides specific to a region downstream of the T-DNA insert, with the

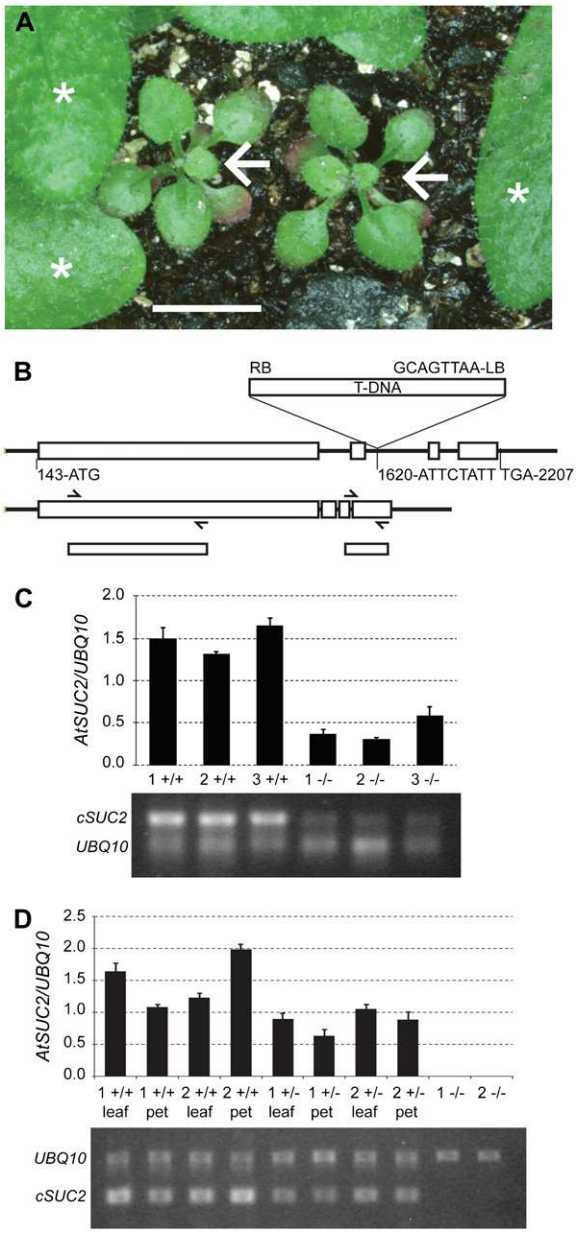

Figure 1. Characterization of the T-DNA insertion mutant SALK_038124. A, Severe stunting and anthocyanin accumulation in homozygous *Atsuc2*::*T-DNA* SALK_038124 plants (*AtSUC2* −/−; arrows) relative to siblings segregating wild type (*AtSUC2* +/+) or heterozygous (*AtSUC2* +/−; leaves marked with asterisks). All plants are the same age. Bar = 5 mm. B, Top, Schematic of the T-DNA insertion site in the second intron of *AtSUC2* (At1g22710) in SALK_038124 with nucleotides flanking the insertion site indicated. Numbering is relative to the start of the 5′ UTR, based on the gene model AT1G22710.1 at http://www.Arabidopsis.org. Bottom, Schematic of the mRNA showing exons spliced together, the approximate binding sites of oligonucleotides used for semiquantitative RT-PCR (from left to right: SUC2F, SUC751R, AtSUC2Ex3Ex4F, and SUC2-3-UTR; see "Materials and Methods" for sequences), and the resulting PCR products. C, Semiquantitative RT-PCR for *AtSUC2* cDNA sequences upstream of the T-DNA insertion site, relative to the *UBQ10* transcript, from leaves of three sibling *AtSUC2* +/+ and *AtSUC2* −/− plants, as indicated (siblings marked 1, 2, and 3). Average and SD values from three PCR replicates are represented in the graph, and below is a representative gel image. D, Semiquantitative RT-PCR for *AtSUC2* sequences downstream of the T-DNA insertion site, relative to the *UBQ10* transcript, from two sibling *AtSUC2* +/+, +/−, and −/− plants (siblings marked 1 and 2). For each *AtSUC2* +/+ and +/− plant, RNA was isolated separately from three leaf blades including the midrib (leaf) and associated petioles (pet) or from whole plants for *AtSUC2* −/−. Average and SD values from three PCR replicates are represented in the graph, and below is a representative gel image.

forward oligonucleotide spanning the exon 3-exon 4 junction, did not produce a product from *AtSUC2* −/− plants, but a robust band was obtained with *AtSUC2* +/+ plants (Fig. 1D). Together, these results show that mutant *AtSUC2* transcripts are less abundant and are missing exons 3 and 4. If translated, the AtSUC2 protein would have 440 of 512 amino acids and would be missing the final two transmembrane domains, an extracellular domain, and the C-terminal cytoplasmic domain. Based on this molecular characterization, and the phenotype similarities to those described previously, it is likely that SALK_038124 harbors a null mutation at the *AtSUC2* locus. Heterozygous *AtSUC2* +/− plants had modestly reduced growth relative to *AtSUC* +/+ plants (see Fig. 3A) and also had less *AtSUC2* mRNA (Fig. 1D).

Design and Testing of *AtSUC2* Cassettes

To assess the role of AtSUC2 in distributing Suc along the transport phloem and throughout the plant, *AtSUC2* cDNA (referred to throughout as *cSUC2* to differentiate from the endogenous locus, *AtSUC2* [At1g22710]) was fused to *CmGAS1p* (Fig. 2A), which drives gene expression specifically in the minor veins of mature leaves (i.e. the collection phloem) and does not promote expression in larger veins or vascular tissue in stems and roots (i.e. transport and release phloem; Haritatos et al., 2000). Two kilobases of the natural *AtSUC2* promoter sequence (*SUC2p*) was used as a positive control (Truernit and Sauer, 1995; Wright et al., 2003). Fusion proteins were desirable, since the visible marker would allow localization of the transporter; however, it was not known if the fusions would be functional for Suc/H^+ symport. Therefore, the fusion genes were subcloned downstream of the yeast (*Saccharomyces cerevisiae*) *ADH1* promoter (Ayre et al., 2002) and tested in yeast prior to generating transgenic plants (Riesmeier et al., 1992; Barker et al., 2000). Efficient [U-^{14}C]Suc uptake was observed in cells harboring *cSUC2* but not in those harboring *cSUC2*::*uidA* or the parent plasmid without *cSUC2* (Fig. 2B). Cells harboring *cSUC2*::*GFP* demonstrated intermediate uptake activity (data not shown). Based on these activity assays in yeast, *cSUC2* was used in plants for complementation assays, and *cSUC2*::*uidA* was used to confirm the expected expression pattern.

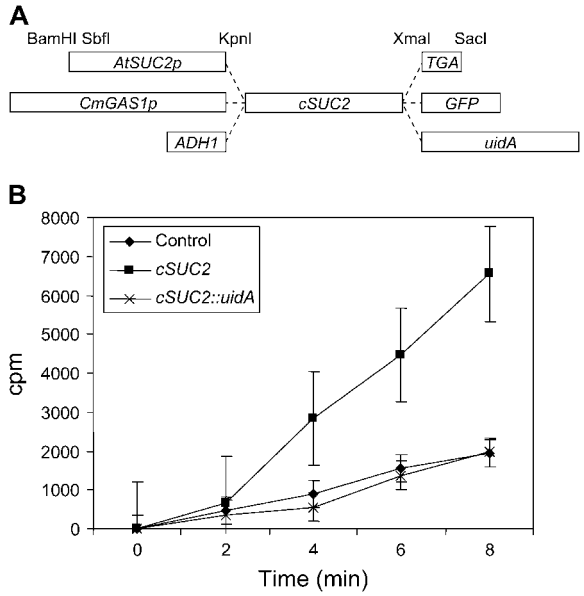

Figure 2. Cassettes used for complementation, and transport activity of fusion proteins in *Saccharomyces cerevisiae*. A, Schematic representation of cassettes for tissue-specific expression of *AtSUC2* cDNA (*cSUC2*) as the native protein and as fusions with reporter enzymes GFP and GUS (encoded by *uidA*). Promoters, fusions, and restriction endonuclease recognition sequences are as indicated; TGA, in-frame stop codon flanked by restriction sites for creating the native AtSUC2 protein. Reporter genes also terminate with a TGA stop codon (data not shown). The schematic is not to scale. B, Uptake of [U-^{14}C]Suc into yeast strain SuSy7-ura3 transformed with an empty vector control (diamonds), *cSUC2* (squares), and *cSUC2*::*uidA* (crosses) expressed from the *ADH1* promoter. Incubation with labeled Suc was terminated at the indicated time points, and incorporation (cpm) was determined by scintillation counting. Average and SD values from three experiments are represented.

Characterization of Complemented Mutants

Homozygous *AtSUC2* −/− plants are unsuitable for transformation by floral dip because of their severe stunting and low fecundity. The binary vectors harboring the *cSUC2* cassettes, therefore, were transformed into heterozygous *AtSUC2* +/− plants, and transgenic progeny (T1) were genotyped as *AtSUC2* +/+, +/−, or −/− by PCR. For each *cSUC2* and *cSUC2*::*uidA* construct, 12 independently transformed lines were identified that, based on a 3:1 segregation ratio for glufosinate ammonium resistance in the subsequent generation, contained T-DNA at a single locus. Tandem copies are possible.

T2 or T3 plants harboring the *cSUC2* and *cSUC2*::*uidA* cassettes, and homozygous *AtSUC2* −/−, were analyzed for vegetative growth at 21 d after germination (Fig. 3A). The independent lines showed growth characteristics ranging from no better than *AtSUC* −/− (data not shown) to not significantly different from *AtSUC2* +/− and *AtSUC* +/+ (Fig. 3A). Homozygous *AtSUC2* −/− plants transformed with *cSUC2*::*uidA* demonstrated poor growth (Fig. 3), as expected based on Suc uptake into yeast cells. Some, however, performed slightly better than uncomplemented mutants, implying that the fusion protein retains some activity. Also, consistent with the activity of *cSUC*::*GFP* in yeast, growth among mutant plants transformed with *cSUC2*::*GFP* was intermediate between *cSUC2* and *cSUC2*::*uidA* plants (data not shown).

The average rosette area of the four most robust *SUC2p-cSUC2* transformants was not significantly different from that of heterozygous plants (Fig. 3; Table I). Lines marked with asterisks in Figure 3 are homozygous for the indicated *cSUC2* cassette, based on 100% resistance to glufosinate ammonium among 32 seedlings. Line KD1039 showed growth not significantly different from wild-type *AtSUC* +/+ (Fig. 3; Table I) and was chosen as a representative line for further study. Root growth was not significantly different from that in wild-type roots at 16 d after germination on sterile Murashige and Skoog (MS) medium with 0% Suc (Table I). A representative *SUC2p*::*cSUC2*::*uidA* plant stained with X-GlcA is shown in Figure 3I, demonstrating staining only in the vascular tissue of mature leaves. In immature leaves, the staining pattern was characteristic of the sink-to-source transition, as described previously for this promoter (Truernit and Sauer, 1995; Wright et al., 2003). None of the 12 *SUC2p*::*cSUC2*::*uidA* lines analyzed deviated from this pattern, and the pattern was consistent whether the plants were segregating *AtSUC2* +/+, +/−, or −/−. Transcript abundance of *cSUC2* in the lamina of KD1039 leaves exceeded *AtSUC2* transcript abundance in the lamina of *AtSUC2* +/+ plants (Fig. 4A). Transcript levels of *cSUC2* in petioles of KD1039 plants were lower than in the lamina, whereas *AtSUC2* levels in the petioles of *AtSUC2* +/+ plants showed greater variation. Petiole and lamina tissues were from the same leaves.

The four most robust lines harboring *CmGAS1p*::*cSUC2* and segregating *AtSUC2* −/− were smaller than *AtSUC2* +/+ and *AtSUC2* +/−; they were also smaller than *AtSUC2* −/− lines complemented by *SUC2p*::*cSUC2* but much larger than *AtSUC2* −/− plants without complementation. All plants represented in Figure 3 supported good seed yield. Line KD1294 was selected as a representative line. Root growth was diminished relative to KD1039 and *AtSUC2* +/+ plants (Table I). The well-documented minor vein-specific expression pattern conferred by *CmGAS1p* was confirmed by X-GlcA staining in plants harboring *CmGAS1p*::*cSUC2*::*uidA* (Fig. 3I). The same staining pattern was observed in all lines whether segregating *AtSUC* +/+, +/−, or −/−.

As an additional test for the absence of *cSUC2* expression in the transport phloem, semiquantitative reverse transcription (RT)-PCR was performed relative to *UBQ10* and compared with *AtSUC2* +/+ and KD1039 plants (Fig. 4). Two different reverse primers were used with AtSUC2Ex3Ex4F to test for consistency. Primer SUC2-3-ORF binds *AtSUC2* and *cSUC2* (Fig. 4A), whereas NospASacR is specific to *cSUC2*

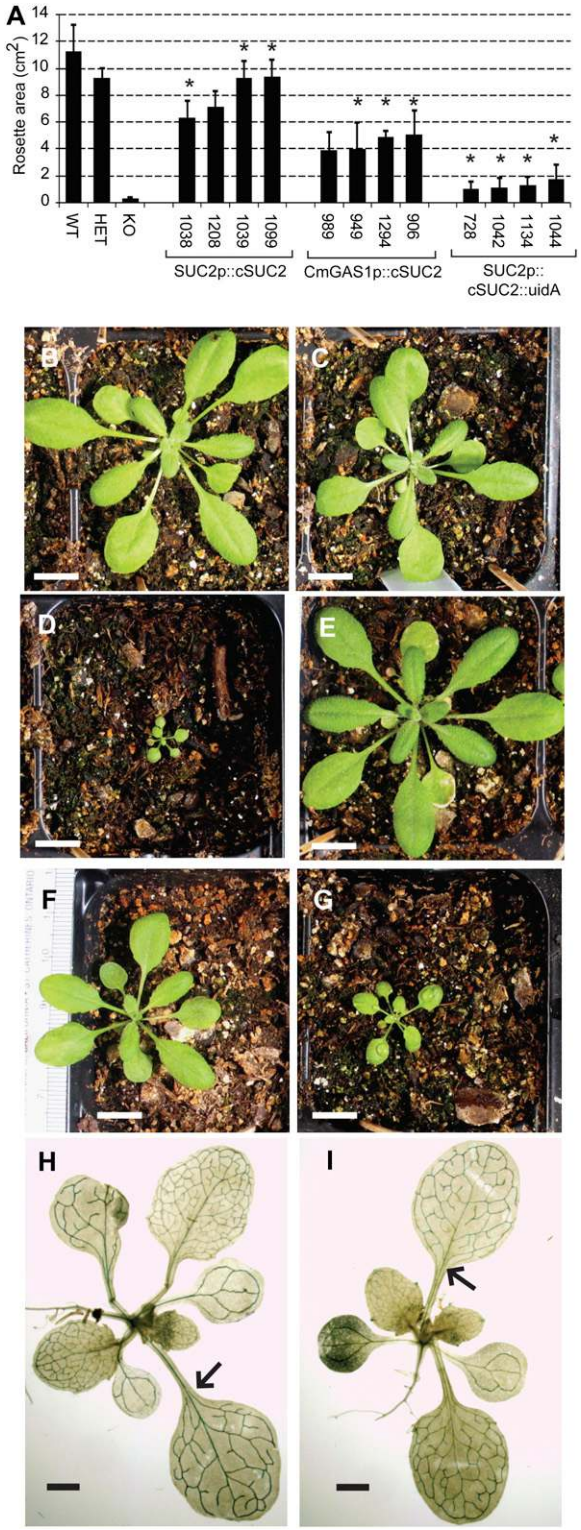

Figure 3. Growth characteristics of *AtSUC2* +/+, +/−, and −/− and *AtSUC2* −/− lines harboring the *cSUC2* cassettes *SUC2p*::*cSUC2*, *CmGAS1p*::*cSUC2*, and *SUC2p*::*cSUC2*::*uidA*. A, Rosette area (cm^2) of 21-d-old *AtSUC2* +/+, +/−, and −/− plants and *AtSUC2* −/− plants independently transformed (indicated by seed stock number) with the indicated *cSUC2* constructs. Variation is expressed as SD; $n = 3$ to 10 sibling plants. Lines homozygous for the *cSUC2* cassettes are indicated with asterisks. B to D, Representative 21-d-old *AtSUC2* +/+ (B), +/− (C), and −/− (D) plants. E to G, Representative 21-d-old *AtSUC2* −/− plants transformed with *SUC2p*::*cSUC2* (E), *CmGAS1p*::*cSUC2* (F), and *SUC2p*::*cSUC2*::*uidA* (G) constructs. Bars in B to G = 1 cm. H and I, X-GlcA staining in source leaves of *AtSUC2* +/− plants expressing *SUC2p*::*cSUC2*::*uidA* (H) and *CmGAS1p*::*cSUC2*::*uidA* (I). Arrows highlight X-GlcA staining in the midrib and petiole in H and the lack of staining in the midrib and petiole in I. Bars in H and I = 1 mm.

(Fig. 4B). In KD1294 plants, transcript was detected in the lamina, where the collection phloem resides, but not in the petiole (Fig. 4) or inflorescence stem tissues (data not shown), which contain transport phloem. PCR products from petioles and stem were not visible after 40 cycles. These results show that *CmGAS1p*::*cSUC2* restores expression only to the collection phloem. In the lamina of KD1294 plants, *cSUC2* transcript abundance was less than that in *AtSUC2* +/+ and KD1039 plants. These lamina tissues samples included the midrib and secondary veins, where *SUC2p* is active but *CmGAS1p* is not. Since *cSUC2* transcript from *CmGAS1p* is only present in a subset of veins (the minor veins), its abundance in the collection phloem is likely underrepresented.

Transient Carbohydrate Distribution in the Leaf

Suc is the predominant transport sugar in Arabidopsis (Haritatos et al., 2000). When Suc is not efficiently transported out of photosynthesizing leaves, soluble sugars and starch accumulate (Schulz et al., 1998; Gottwald et al., 2000). To assess the effect of the different *cSUC2* expression patterns on carbon partitioning, the distribution of the major forms of transport and storage carbohydrate was analyzed among *AtSUC* +/+, +/−, −/−, and the complemented lines KD1039 and KD1294 (Table II) at 30 d after germination. Levels of soluble sugar were similar in *AtSUC* +/+, +/−, and KD1039 plants, but starch levels in *AtSUC2* +/− and KD1039 were roughly double that of *AtSUC2* +/+. KD1294 plants had two to three times more soluble sugar than *AtSUC2* +/+, +/−, and KD1039 plants, whereas starch was 2.5- to 3-fold higher than in *AtSUC2* +/− and KD1039 plants and nearly 7-fold higher than in *AtSUC2* +/+ plants. *ASUC2* −/− plants, remarkably, had 20-fold or greater levels of soluble sugar and starch, relative to *AtSUC2* +/+ plants.

If AtSUC2 is involved in efflux from the transport phloem, then its absence might contribute to reduced carbohydrate in leaf petioles, since Suc passing along the transport phloem would not be lost to lateral tissues. Alternatively, if AtSUC2 is not involved in efflux but is required for retrieval, increased levels of carbohydrate in petioles would be expected. Transient carbohydrate levels in lamina (with midrib removed) and petiole sections, therefore, were measured and compared among lines. *AtSUC2* +/+ and KD1039 did

Table I. *Measurement of rosette area at 21 d after germination among independently transformed lines grown on potting mix, and root length of representative lines grown for 16 d on sterile MS medium without Suc*

Average rosette areas are shown for *AtSUC2* +/+, +/−, and −/− plants, the four most robust lines combined (Fig. 3A), and the indicated representative line. Root length of representative lines is shown on sterile MS medium without Suc at 16 d after germination. Variation is expressed as SD; $n = 3$ to 10 siblings.

Plant Line	Rosette Area		Root Length
	cm^2		*cm*
AtSUC2 +/+	11.21 ± 1.98		5.23 ± 0.25
AtSUC2 +/−	9.22 ± 0.76		n.d.[b]
AtSUC2 −/−	0.28 ± 0.08[a]		0.15 ± 0.10[a]
	Four Lines Combined	Representative Line	Representative Line
SUC2p::cSUC2	8.00 ± 1.54[a]	9.34 ± 1.26 (KD1039)	5.60 ± 0.70 (KD1039)
CmGAS1p::cSUC2	4.45 ± 0.58[a,c]	4.83 ± 0.49[a,c] (KD1294)	4.53 ± 0.35[a] (KD1294)
SUC2p::cSUC2::uidA	1.25 ± 0.34[a,c]	1.29 ± 0.56[a,c]	n.d.

[a]Student's *t* test, $P < 0.05$, relative to wild-type *AtSUC2/AtSUC2*. [b]n.d., Not determined. [c]Student's *t* test, $P < 0.05$, relative to heterozygous *AtSUC2/Atsuc2::T-DNA*.

not show significantly different levels of Glc, Fru, or Suc in the lamina or the petiole (Table III). Starch similarly showed no difference in the petiole samples, but in the lamina, starch was elevated in KD1039, as was observed when whole leaves were sampled (Table II). KD1294 carbohydrate levels in the lamina were greater than those observed in the whole leaf samples (Table II), possibly because the midrib, which contributes fresh weight but would contain carbohydrate levels similar to the petiole, was removed. Petioles of KD1294 contained higher levels of sugar and starch than KD1039 and *AtSUC2* +/+ plants, supporting a role for AtSUC2 in retrieval.

Transport Efficiency of ^{14}C-Labeled Sugars

To assess movement along the transport phloem in intact plants, [U-^{14}C]Suc was applied to the distal tip of mature leaves of *AtSUC2* +/+, *AtSUC2* −/−, KD1039, and KD1294, and migration through the petiole was monitored by autoradiography. [U-^{14}C]Suc was applied at 0.5 mM to keep apoplastic Suc in the physiological range (Ayre et al., 2003). Leaves were harvested at time points ranging from 1 min to 4 h after labeling. Release of radiolabeled sugars from the transport phloem to flanking tissues without retrieval may have resulted in a diffuse signal, but this was not observed (Fig. 5). The same pattern was obtained for *CmGAS1p::cSUC2* and controls, showing that detectable loss to lateral tissues along the petiole did not occur. Transport of label along the petiole of *AtSUC2* −/− plants was not observed.

To assess the efficiency of photoassimilate transport out of the leaf, excised leaves were photosynthetically labeled with $^{14}CO_2$, and phloem sap was collected over 20 h by an EDTA exudation method (Turgeon and Medville, 2004). At the end of the exudation experiment, the amount of isotope exuded from the leaves was determined relative to the amount retained by the leaves in soluble and insoluble fractions (Table IV, top three entries). Leaves of *AtSUC2* +/+ and KD1039 plants had similar distributions in exuded and retained fractions. Relative to *AtSUC2* +/+, KD1294 had reduced levels of exudation after 20 h. This line also incorporated more ^{14}C-labeled photosynthates into the insoluble fraction. These results further show that phloem transport is compromised in *CmGAS1p::cSUC2* lines but that the absence of *AtSUC2* along the transport phloem has only a modest effect on phloem transport. None of the lines showed a significant difference in the percentage of label retained in the leaf as soluble components. In a second series of exudation experiments, *AtSUC2* +/+ plants were compared with *AtSUC2* −/− plants (Table IV, bottom two entries). Exudate was collected from the stem below the cotyledonary leaves of the *AtSUC2* −/− plants rather than from petioles. Surprisingly, the ^{14}C distribution and exudation rate in the *AtSUC2* −/− samples showed little difference from the *AtSUC2* +/+ samples, and this may point to an alternative transport mechanism in Arabidopsis (see "Discussion").

DISCUSSION

The transport phloem has characteristics of both collection and release phloem: sugars and nutrients are released to supply the metabolic needs of the lateral tissues and to enter transient storage reserves, but leaked sugars and those from lateral reserves also need to be retrieved (van Bel, 2003). Suc retrieval is attributed to Suc symporters that are expressed along the transport phloem, but nutrient release has remained more enigmatic. Under extreme conditions of low sink strength and abundant photoassimilate in the phloem, symplastic unloading to lateral tissues through plasmodesmata may occur (Hayes et al., 1987). More commonly, however, unloading is across the membrane to the apoplast (Aloni et al., 1986;

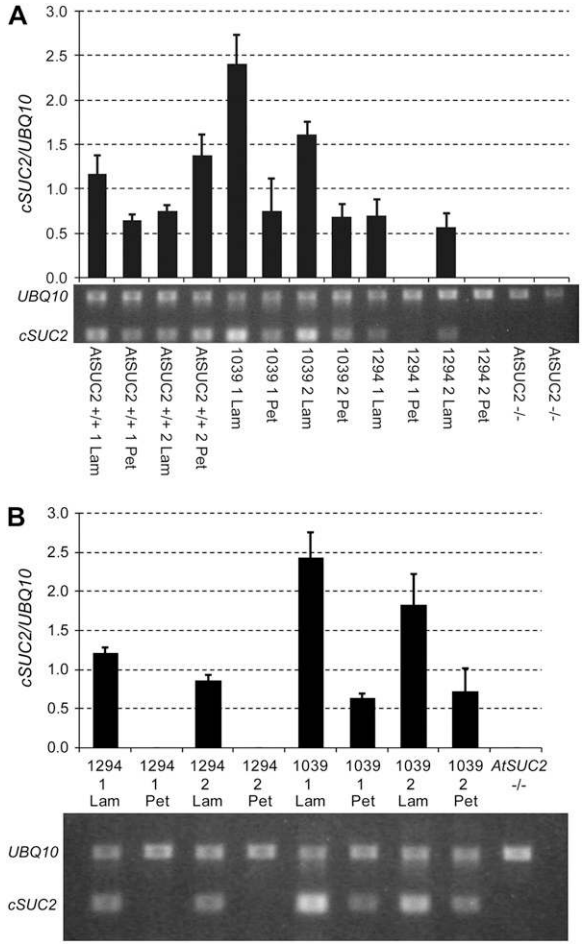

Figure 4. Semiquantitative RT-PCR transcript analysis comparing *AtSUC2* and *cSUC2* expression levels in lamina samples that included the midrib (Lam) and petioles (Pet). A, *AtSUC2* and *cSUC2* transcript abundance relative to *UBQ10* from two sibling plants (siblings marked 1 and 2) of *AtSUC2* +/+, *SUC2p*::*cSUC2* (1039), *CmGAS1p*::*cSUC2* (1294), and *AtSUC2* −/− plant (whole plant sample), as indicated, using primers AtSUC2Ex3Ex4F and SUC2-3-ORF. B, cSUC2 transcript abundance relative to *UBQ10* from two sibling plants (siblings marked 1 and 2) of *CmGAS1p*::*cSUC2* (1294), *SUC2p*::*cSUC2* (1039), and one *AtSUC2* −/− plant (whole plant sample), as indicated, using primers AtSUC2Ex3Ex4F and NospASacR. Average and SD values from three PCR replicates are represented in the graphs, and below each graph is a representative gel image.

Minchin and Thorpe, 1987; Grimm et al., 1997), which is consistent with ultrastructural and dye-coupling experiments that demonstrate symplastic isolation of the transport phloem from lateral tissues (Kempers and van Bel, 1997; Kempers et al., 1998). How Suc is lost to the apoplast is uncertain, as a clear efflux carrier has not emerged; however, as described in the introduction, there is circumstantial evidence that the same symporter(s) involved in retrieval may also be involved in efflux.

Here, we address the role of the AtSUC2 Suc/H^+ symporter in mediating Suc distribution along the transport phloem by first characterizing the Arabidopsis line SALK_038124, which contains a T-DNA insertion in the *AtSUC2* second intron. Transcript corresponding to sequences upstream of the insertion site was detected at reduced levels relative to the wild type, suggesting that transcript stability is compromised. Transcript corresponding to sequence downstream of the insert was not detected (Fig. 1). Any translated protein would be missing 72 C-terminal amino acids, corresponding to two membrane-spanning domains, an extracellular domain, and the C-terminal cytoplasmic domain (Bush, 1999; Gottwald et al., 2000). Morphologically, these mutants are identical to three previously characterized insertion mutants, one of which is in the first exon and would have disrupted any AtSUC2 protein after amino acid 162 in the fourth transmembrane domain (Gottwald et al., 2000). Based on these identical phenotypes, we believe that SALK_038124 harbors an *Atsuc2* knockout.

Heterozygous *AtSUC2* +/− plants showed a modest growth reduction, accumulated starch, and had reduced *AtSUC2* transcript relative to the wild type, implying that gene copy number influences plant productivity. This was unexpected, as expression of Suc/H^+ symporters involved in phloem transport has a broad dynamic range to match the needs of the plant with physiological and/or environmental conditions: the proteins turn over rapidly, and the genes may be highly expressed or virtually silent in response to sugar signaling and light conditions (Kuhn et al., 1997; Matsukura et al., 2000; Vaughn et al., 2002; Wright et al., 2003). It would have been reasonable to assume that a single-copy gene could compensate for the missing copy by increasing expression, especially under standard laboratory conditions that avoid extreme conditions. Rather, these observations support a model in which phloem-loading capacity is directly proportional to transcriptional activity (Vaughn et al., 2002). Accelerated growth has not been observed in *AtSUC2* +/+ or +/− plants when *cSUC2* is expressed from phloem-specific promoters (A.C. Srivastava and B.G. Ayre, unpublished data).

The role of *AtSUC2* in mediating Suc distribution along the transport phloem was further characterized by tissue-specific complementation in *AtSUC2* −/− plants. Growth of the most robust *SUC2p*::*cSUC2* plants was not significantly different from *AtSUC2* +/+ but more closely resembled *AtSUC2* +/− plants (Fig. 3; Table I), and KD1039 showed starch accumulation, implying that full complementation was not achieved. Isolating more than 12 independent lines may identify a fully complemented line. However, *cSUC2* transcript levels in KD1039 lamina samples exceeded those of *AtSUC2* in *AtSUC2* +/+ lamina, suggesting that the effect is posttranscriptional. One possibility is that the partial transcript or protein (if produced) from the endogenous gene may interact negatively with transcript or protein derived from *cSUC2*.

AtSUC2 activity was complemented specifically in the collection phloem by expressing the cDNA from *CmGAS1p* in *AtSUC2* −/− plants. In this manner, we

Table II. *Sugar and starch in whole leaves (blade and petiole) of the indicated lines*

Accumulation of transient carbohydrates in mature leaves of the indicated lines was measured to assess whether photoassimilate was efficiently transported out of leaves. The first three adult leaves from a single plant were pooled for extraction, and carbohydrate levels were measured in three (*AtSUC2* +/−) or five siblings. All values are nanomoles per milligram fresh weight, and starch is expressed as Glc equivalents.

Line	Glc	Fru	Suc	Starch	Total
AtSUC2 +/+	0.94 ± 0.54	0.35 ± 0.22	1.56 ± 0.72	29.2 ± 7.1	32.5 ± 7.8
AtSUC2 +/−	1.44 ± 0.65	0.31 ± 0.06	2.42 ± 1.07	80.4 ± 11.8[a]	84.5 ± 13.6[a]
AtSUC2 −/−	23.2 ± 7.2[a]	8.23 ± 2.14[a]	28.0 ± 6.1[a]	719 ± 114[a]	779 ± 127[a]
SUC2p::cSUC2 KD1039	0.66 ± 0.14	0.22 ± 0.09	2.28 ± 0.40	72.2 ± 11.8[a]	75.3 ± 12.1[a]
CmGAS1p::SUC2 KD1294	2.67 ± 0.96[a]	0.49 ± 0.19[a]	4.94 ± 1.44[a]	201 ± 34[a]	209 ± 36[a]

[a]Student's *t* test, $P < 0.05$, relative to *AtSUC2* +/+.

restored the phloem-loading function of *AtSUC2* while retaining mutant characteristics in the transport and release phloem, in order to isolate the role of AtSUC2 in efflux and retrieval. Although the expression pattern conferred by *CmGASp* is well established (Haritatos et al., 2000), confirmation was important for accurate interpretation of our results. X-GlcA staining was not observed in larger veins of leaves or in stem tissues of *CmGAS1p::sSUC2::uidA* plants, and *cSUC2* transcript was not detected in KD1294 stem and petiole tissue by semiquantitative RT-PCR but was readily apparent in KD1039 (Figs. 3 and 4). Qualitative assessment of X-GlcA staining showed comparable intensity in the minor veins of *CmGAS1p::cSUC2::uidA* and *SUC2p::cSUC2::uidA cSUC2* lines, but semiquantitative RT-PCR showed less *cSUC2* transcript in the leaf blades of KD1294 than in KD1039 and AtSUC2 +/+. The tissues used for RNA extraction, however, contained the midrib and secondary veins, where *SUC2p* expresses strongly and *CmGAS1p* does not. Therefore, it is not surprising that *CmGAS1p::cSUC2* transcripts are underrepresented.

The growth of *CmGAS1p::cSUC2* plants was reduced relative *AtSUC2* +/+, +/−, and −/− plants complemented with *SUC2p::cSUC2*, but it was sufficiently robust for the plants to complete their life cycle (Fig. 3). The lamina and petiole of KD1294 leaves accumulated sugar and starch relative to *AtSUC2* +/+ and KD1039 (Tables II and III). In the lamina, this could be caused by weaker phloem loading in the minor veins, or efflux from the transport phloem in larger veins without *AtSUC2*-mediated retrieval, or a combination of the two. Higher levels of sugar and starch in the petiole argue that efflux from the transport phloem occurs but retrieval is compromised in the absence of AtSUC2. Some photosynthesis is likely along the petiole, and failure to retrieve this photoassimilate would also contribute to higher levels of transient carbohydrate. Reduced exudation of ^{14}C from cut petioles and elevated levels in the insoluble fraction of KD1294 plants, relative to *AtSUC2* +/+ and KD1039, similarly support efflux without retrieval along the transport phloem. If, on the other hand, AtSUC2 participated in efflux, less sugar and starch in

Table III. *Sugar and starch in the lamina (excluding midrib) and petiole of the indicated lines*

Transient carbohydrates in the lamina and petiole of the indicated lines were measured to assess the efficiency of transport out of the leaf and along the transport phloem. The first three adult leaves from a single plant were pooled for extraction, and carbohydrate levels were measured in three to five siblings. All values are nanomoles per milligram fresh weight, and starch is expressed as Glc equivalents.

Representative Line	Carbohydrate	Lamina	Petiole
AtSUC2 +/+	Glc	2.28 ± 0.95	0.51 ± 0.02
	Fru	0.80 ± 0.36	0.14 ± 0.03
	Suc	1.72 ± 0.76	0.35 ± 0.07
	Starch	59.5 ± 5.0	8.28 ± 3.68
	Total	64.3 ± 4.4	9.28 ± 3.79
SUC2p::cSUC2 KD1039	Glc	1.40 ± 0.42	0.53 ± 0.15
	Fru	0.42 ± 0.12	0.12 ± 0.02
	Suc	1.40 ± 0.40	0.35 ± 0.07
	Starch	84.6 ± 18.2[a]	12.02 ± 3.64
	Total	87.8 ± 18.2[a]	13.02 ± 3.60
CmGAS1p::cSUC2 KD1294	Glc	13.00 ± 2.7[a]	1.36 ± 0.17[a]
	Fru	3.78 ± 1.22[a]	0.24 ± 0.03[a]
	Suc	5.76 ± 0.52[a]	0.83 ± 0.17[a]
	Starch	639.5 ± 61.9[a]	37.1 ± 7.0[a]
	Total	662.0 ± 65.8[a]	39.5 ± 7.2[a]

[a]Student's *t* test, $P < 0.05$, relative to the wild type.

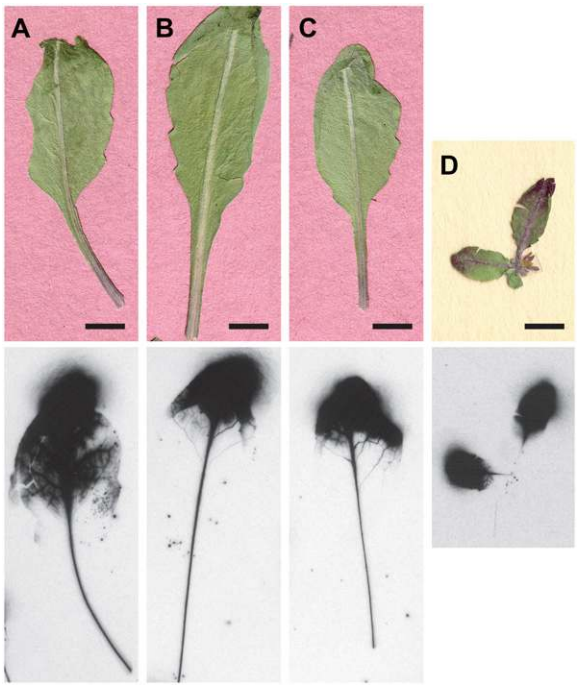

Figure 5. Transport of [U-^{14}C]Suc along the midrib and petiole in intact plants at 1 h after application to the distal tip. A, *AtSUC2* +/+ leaf. B, KD1039 leaf. C, KD1294 leaf. D, *AtSUC2* −/− whole plant. Freeze-dried and pressed leaves are shown at top and autoradiographs are shown at bottom. Plants in A to C were 30 d old, when *AtSUC2* −/− was still very small; the plant in D was 70 d old.

the petiole and improved exudation in KD1294 would have been expected. Furthermore, if AtSUC2 was involved in efflux from the transport and release phloem, root growth, and indeed, development of all sinks, should have been stunted more than what was observed, as the apoplastic pathway for carbon distribution would have been affected.

If, in the absence of retrieval, Suc loss to the apoplast was extensive, autoradiography may have detected a diffuse signal in the midrib and petiole after labeling KD1294 plants with [U-^{14}C]Suc (Fig. 5). As a precedent, the rate of loss along the stem of *P. vulgaris* was measured at 6% cm^{-1} in the absence of the retrieval (Minchin and Thorpe, 1987). The signal along the midrib and petiole of KD1294, however, was the same as the pattern in KD1039 and *AtSUC2* +/+, and we interpret this to mean that Suc retention in the phloem is efficient in the absence of retrieval. This is not surprising, since, although loss in *P. vulgaris* was 6% cm^{-1}, the rate of loss in stems of *Cyclamen persicum* was only 0.6% cm^{-1} (Grimm et al., 1997), suggesting substantial variation between species.

Therefore, AtSUC2 is not required for efflux in the transport and release phloem, but its retrieval function likely participates in fine-tuning whole plant carbon partitioning. Surprisingly, the loading function of AtSUC2 in the collection phloem also does not appear to be "essential," since, although extremely stunted, *AtSUC2* −/− plants do grow, showing that photoassimilate distribution is occurring. We believe that the mutation in SALK_038124 does not retain AtSUC2 activity, as argued above, and although the Arabidopsis Suc/H$^+$ symporter family has nine members, none appears to have characteristics that could substitute for *AtSUC2* (Sauer, 2007; Sivitz et al., 2007, 2008). SUT4 expresses in leaf veins, but it appears to play its major role in the release phloem (Chincinska et al., 2008). The hydrostatic pressure gradient required for phloem transport in *AtSUC2* −/− plants may rely more on other solutes, such as K$^+$ and alternative forms of fixed carbon. For example, earlier work showed increases in phloem K$^+$ levels associated with decreased Suc availability (Smith and Milburn, 1980), and more recently, K$^+$ channels were localized in the phloem of Arabidopsis (Deeken et al., 2000; Lacombe et al., 2000). Other sugars, such as raffinose family oligosaccharides (Turgeon and Gowan, 1990), sugar alcohols (polyols; Noiraud et al., 2001), and hexose sugars (van Bel and Hess, 2008), all function as transport sugars in various species, and in Arabidopsis specifically, raffinose is found in phloem sap (Haritatos et al., 2000) and a polyol transporter, *AtPLT5*, expresses in phloem cells (Klepek et al., 2005). The contribution of these sugars to phloem transport may be elevated in *AtSUC2* −/− plants.

Another intriguing possibility is that phloem loading, the expenditure of energy to load solute against a

Table IV. *Percentage of ^{14}C-labeled photosynthate exuded from cut petioles and retained in the leaf at 20 h after photosynthetic labeling with $^{14}CO_2$*

Four mature adult leaves were excised and photosynthetically labeled with $^{14}CO_2$. Phloem exudation into EDTA-containing solution was collected and analyzed by scintillation counting. Label remaining in leaves in soluble and insoluble fractions was also established, and label distribution is expressed as a percentage of the total. Experiments in the top and bottom portions of the table were carried out on different days and with different plants. Average and SD values are from four (top three entries) or three (bottom two entries) sibling plants.

Line	Cumulative Percentage ^{14}C Exudation					Soluble Residual	Insoluble Residual
	0 h	2 h	4 h	9 h	20 h		
AtSUC2 +/+	0.0 ± 0.0	20.8 ± 4.1	36.7 ± 6.5	56.4 ± 6.2	70.1 ± 6.2	19.4 ± 4.9	10.5 ± 2.2
KD1039	0.1 ± 0.2	16.6 ± 5.3	31.4 ± 8.7	52.8 ± 6.5	66.5 ± 5.7	21.4 ± 1.8	12.1 ± 5.3
KD1294	0.1 ± 0.0	19.3 ± 4.1	29.9 ± 6.2	45.7 ± 6.8	59.4 ± 5.0[a]	18.7 ± 4.1	21.9 ± 3.1[a]
AtSUC2 +/+	0.0 ± 0.0	30.0 ± 2.9	47.2 ± 4.9	63.5 ± 3.7	75.3 ± 2.5	17.2 ± 0.8	7.5 ± 2.5
AtSUC2 −/−	0.0 ± 0.0	16.3 ± 5.8[a]	31.3 ± 10.2	52.2 ± 9.4	73.6 ± 3.8	18.1 ± 1.6	8.3 ± 2.7

[a]Student's *t* test, $P < 0.05$, relative to *AtSUC2* +/+, performed separately on different experiments.

thermodynamic gradient, is not essential for phloem transport in Arabidopsis. Turgeon and Medville (1998) showed that willow (*Salix* spp.) does not phloem load but instead has its highest solute concentration in mesophyll cells, and this correlates with a relatively high number of plasmodesmata connecting mesophyll and minor veins to permit diffusion down a concentration gradient to the phloem. Arabidopsis minor veins have a lower plasmodesmata density than willow, but greater than tobacco, which is an archetype for loading Suc from the apoplast (Haritatos et al., 2000). Since *AtSUC2* −/− plants accumulate high levels of sugar and have leaf vein morphology compatible with symplastic transport, it is feasible that the hydrostatic pressure gradient driving source-to-sink transport is initiated in the mesophyll. Our radiolabeling experiments support this hypothesis. Adding [U-^{14}C]Suc to *AtSUC2* −/− leaves did not result in phloem transport, presumably because the sugar was not loaded into the minor veins (Fig. 5). However, photosynthetic labeling did result in substantial label in phloem exudates from *AtSUC2* −/− stems. Symplastic transport from the sites of photosynthesis in the mesophyll to the phloem, followed by exudation, would explain this discrepancy.

MATERIALS AND METHODS

Plasmid Construction

Plasmid construction was by standard procedures (Sambrook and Russel, 2001; Ausubel et al., 2002) using *Escherichia coli* XL1-Blue (Stratagene) as the host strain. Restriction endonucleases were from New England Biolabs, oligonucleotides were obtained from Invitrogen, and *Pfu*I Ultra proofreading DNA polymerase (Stratagene) was used for PCR amplification of plasmid components. All clones incorporating a PCR product were sequenced to ensure accuracy (SeqWright).

The 1,536-bp cDNA of Arabidopsis (*Arabidopsis thaliana*) *AtSUC2* (At1g22710) was amplified from pUNI clone U10762 (Arabidopsis Biological Resource Center; Yamada et al., 2003) using gene-specific oligonucleotides AtSUC25 (5′-TTCAAGGTACCAAATATGGTCAGCCATCCAATG-3′; *Kpn*I site underlined) and AtSUC23 (5′-TTCAAGAGCTCATACCCGGGGATGAAATCCCATAGTAGCTTTG-3′; *Sac*I and *Xma*I sites underlined). The cDNA was purified with the Wizard SV gel and PCR clean-up system (Promega), digested with *Kpn*I and *Sac*I, and ligated into the same sites of pGem::*GUT*::*T7CO*, which is identical to pUC::*GUT*::*T7CO* but with a pGEM3zf+ backbone replacing the pUC19 backbone (Ayre and Turgeon, 2004), creating pGEM::*CmGAS1p*::*cSUC2*. Two kilobases of *AtSUC2* promoter was PCR amplified using oligonucleotides AtSUC2p5 (5′-TCAATCCTGCAGGTCGACGGT-3′; *Pst*I/*Sbf*I site underlined) and AtSUC2p3 (5′-TCAATGGTACCTTCCCGGGAT-3′; *Kpn*I site underlined), digested with *Pst*I and *Kpn*I, and ligated into the same sites of pGEM::*CmGAS1p*::*cSUC2* to create pGEM::*SUC2p*::*cSUC2*. These promoter::*cSUC2* cassettes were then subcloned into pGPTV-Bar (Becker et al., 1992), as is or as fusions with *GFP* and *uidA*, and electroporated into *Agrobacterium tumefaciens* strain GV3101mp90 as described (Ayre and Turgeon, 2004).

cSUC2, *cSUC2*::*GFP*, and *cSUC2*::*uidA* cassettes were obtained by digesting the above vectors with *Kpn*I and *Sac*I and ligating into the same sites of pRS424::ADH-MCS, a yeast shuttle vector created by annealing and ligating two partially complementary oligonucleotides (5′-GATCCGGTACCATGGCCCGGGCTCACCACCACCACCACCACTGAGCTCGAATTCTGCA-3′; *Bam*HI half site, *Kpn*I, *Sac*I, and *Pst*I half site, respectively, underlined; and 5′-GAATTCGAGCTCAGTGGTGGTGGTGGTGAGCCCGGGCCATGGTACCG-3′; *Pst*I half site, *Sac*I, *Kpn*I, and *Bam*HI half site, respectively, underlined) into p2ATΔP5-GVP (Ayre et al., 2002) digested with *Bam*HI and *Pst*I to compare the activity of native AtSUC2 and AtSUC2 fusion proteins in bakers' yeast (*Saccharomyces cerevisiae*).

Expression of *AtSUC2* in Bakers' Yeast and Transport Test

Yeast strain SuSy7-URA (Barker et al., 2000) was transformed with the yeast shuttle vectors described above and selected on synthetic dropout (SD) medium lacking Trp (Ayre et al., 2002). Cultures were grown to logarithmic phase in 10 mL of SD-Trp medium at 30°C and 250 rpm. A total of 5×10^8 cells were harvested for each strain, washed, and resuspended in 1 mL of suspension buffer (25 mM MES, pH 4.4, 1 mM Suc, 6.7 g L^{-1} Bacto yeast nitrogen base without amino acids, 2 g L^{-1} yeast SD medium supplement [catalog no. Y2001; Sigma-Aldrich], 20 mg L^{-1} adenine, uracil, Trp, and His, and 100 mg L^{-1} Leu). [U-^{14}C]Suc (MP Biochemicals) uptake was determined essentially as described by Sauer and Stolz (1994). Harvested cells supplemented with [U-^{14}C]Suc (1 mM, 30 KBq mL^{-1}) were incubated at 30°C, and the reaction was stopped by removing 200 μL to tubes chilled on ice at time points 0, 2, 4, 6, and 8 min. The cell suspensions were passed through disposable filter funnels with glass fiber filters (GF/C; Whatman), and the retained cells were washed three times with 15 mL of ice-cold water. Radioactivity associated with the cells on the filters was determined by liquid scintillation counting (Beckman; LS6000IC).

Plant Material

Seeds of T-DNA insertional mutagenesis lines SALK_087046, SALK_001331, and SALK_038124 were obtained through the Arabidopsis Biological Resource Center (Alonso et al., 2003). Twelve seedlings of each line were screened for the presence of the mutagenizing T-DNA using a T-DNA-specific oligonucleotide (LB SALK, 5′-GCGTGGACCGCTTGCTGCAACT-3′) and *AtSUC2*-specific oligonucleotides upstream and downstream of the insert (for SALK_087046 and SALK_001331, PR1F [5′-AACCGCAACCGCAGCCTCTAAG-3′] and PR1R [5′-CCTAGGGAAAGTCCTGTGGAAGAA-3′]; for SALK_038124, PR25 [5′-TTCTTCCACAGGACTTTCCCTAGG-3′] and PR23 [5′-CATACTTAGGGGAAAAGGCTTGTC-3′]). The PCR product corresponding to the T-DNA insert in SALK_038124 was sequenced to confirm the insertion site.

Heterozygous plants (*AtSUC2*/*Atsuc2*::*T-DNA*) were transformed with the promoter-cDNA constructs by the floral dip procedure (Clough and Bent, 1998). T1 generation seeds were sown on SunGro Metro-Mix 366 in 3.5-inch-square pots at approximately 1,000 seeds per pot and stratified for 72 h. Plants were then transferred in a controlled-environment chamber (Percival AR 95 L; Percival Scientific) at 110 to 150 μmol photons m^{-2} s^{-1}, 14 h of light at 22°C, and 10 h of dark at 19°C. Transgenic seedlings were selected by spray application of glufosinate ammonium (20 mg L^{-1}; Finale; Farnam Companies) for 7 d.

Resistant plants were genotyped as *AtSUC2*/*AtSUC2* (designated *AtSUC2* +/+), *AtSUC2*/*Atsuc2*::*T-DNA* (designated *AtSUC2* +/−), or *Atsuc2*::*T-DNA*/*Atsuc2*::*T-DNA* (designated *AtSUC2* −/−) by PCR using the RED Extract-N-Amp plant PCR kit (Sigma-Aldrich) according to the manufacturer's instructions. *AtSUC2*-specific oligonucleotides were AtSUC2F1054 (5′-GGATTGGTCGGAAATTGGGAGGAG-3′) and AtSUC2IVS1210 (5′-CGCGTATATATGGTCACTCAAACG-3′), and the T-DNA-specific oligonucleotide was LB280 (5′-GATTTCGGAACCACCATCAAACAGG-3′). The cycling parameters were 15 s of denaturation at 94°C, 15 s of annealing at 72°C and dropping 1°C every cycle for 12 cycles, and 1 min of elongation at 72°C, followed by 30 additional cycles with annealing at 60°C. Glufosinate ammonium-resistant T1 seedlings segregating *AtSUC2* +/− were grown to seed, and glufosinate ammonium-resistant homozygous *AtSUC2* −/− plants were selected from the T2 generation. Ultimately, 12 or more lines independently transformed with the *AtSUC2* cDNA constructs and segregating homozygous knockout at the genomic locus were obtained from either the T1 or T2 generation.

For growth analysis, seeds from the 12 independent lines for each construct (i.e. T2 or T3 generation) were germinated in individual cells of a 36-cell flat (T.O. Plastics), and rosettes were digitally photographed at 21 d after germination. This was just before the transition to flowering, so all aerial growth was represented in rosette surface area. Rosette surface area (square centimeters per plant) was measured with ImageJ version 1.38x (Rasband, 2007). GUS staining was performed on 14-d-old whole plants as described using 3 mM potassium ferricyanide and ferrocyanide to limit diffusion of GUS reaction products (Ayre and Turgeon, 2004).

Transcript Analysis

Total RNA was isolated from leaf lamina (including midrib), petioles, stems, or whole plants (*AtSUC2* −/−), as indicated, using Trizol (Invitrogen),

according to the manufacturer's instructions. Total RNA samples were treated with RNase-free DNaseI and purified again with Trizol. A total of 500 ng of total RNA was reverse transcribed in the presence of RNase-OUT (Promega) with random hexamer oligonucleotides and SuperScript III reverse transcriptase (Invitrogen) according to the manufacturer's instructions. For semiquantitative PCR, 1 μL of cDNA was amplified in the presence of 200 μM of each dNTP and 200 nM of each primer in 25-μL reactions with REDTaq Genomic DNA Polymerase (Sigma) and supplied buffer. Cycling parameters were 94°C for 10 s, 60°C for 15 s, and 72°C for 50 s. Twenty, 30, and 40 cycles (in separate tubes) were tested for increasing band intensities, and three replicates of 30 cycles were used to quantify band intensity with ImageJ (Rasband, 2007) by resolving 5 to 10 μL on 1.5% agarose gels. Transcript abundance was relative to *UBQ10* (encoding ubiquitin), using oligonucleotides UBQ1 (5′-GATCTTTGCCGGAAAACAATTGGAGGATGGT-3′) and UBQ2 (5′-CGACTTGTCATTAGAAAGAAAGAGATAACAGG-3′; Weigel and Glazebrook, 2002). Oligonucleotides specific to *AtSUC2* sequences upstream of the T-DNA insert were SUC2F (5′-ACAGTTCGGTTGGGCTTTACAGTTATCTC-3′) and SUC751R (5′-TTGGAGGCTTTTCCATCGGCTGTTGGCTCTG-3′). Oligonucleotides specific to *AtSUC2* sequences downstream of the T-DNA insert were AtSUC2Ex3Ex4F (5′-TAGCCATTGTCGTCCCTCAGATG-3′; corresponding to exon 3, except for the last three nucleotides, which are in exon 4) and SUC2-3-UTR (5′-GAGAGAAAGAGAGCCAAACAACCACTG-3′), which is in the *AtSUC2* 3′ untranslated region (UTR). NospASacR (5′-GTTGAACGATCGGGGAAATTCGAGC-3′) is specific for the nopaline synthase 3′ UTR downstream of *cSUC2* and was used with AtSUC2Ex3Ex4F. SUC2-3-ORF (5′-ATGAAATCCCATAGTAGCTTTGAAGG-3′) amplifies both *AtSUC2* and *cSUC2* and was used with AtSUC2Ex3Ex4F.

Transient Carbohydrate Analysis

AtSUC2 +/+, +/−, −/−, KD1039, and KD1294 were grown for 30 d under the conditions described above. The first three adult leaves from siblings (n = 3–5) were excised at the stem, and fresh weights of whole leaf, lamina (leaf blade minus the midrib), and petioles were established. All tissues were collected between 4 and 6 h into the light period, with plants removed from the chamber immediately before sampling. Tissues were immersed in 300 μL of ice-cold MCW extraction solution (methanol:chloroform: water, 12:5:3) containing 100 μM lactose as a standard and kept on ice until all samples were collected. The samples were extracted at 50°C for 15 min, and the extraction was repeated two more times in MCW without lactose. Extracts were combined and phases separated by the addition of 0.6 volumes of water. The methanol:water phase was reduced to approximately 200 μL in a vacuum centrifuge, and the neutral fraction was eluted from a column consisting of AG 50W-X4 cation-exchange resin (H^+ form; Bio-Rad), polyvinyl polypyrrolidone (Sigma-Aldrich), and AG 1-X8 anion-exchange resin (formate form; Bio-Rad), 250-, 100-, and 250-μL bed volumes, respectively (top to bottom), and washed with 1.0 mL of water. The collected flow-through was filtered through a 0.22-μm nylon HPLC filter (Corning-Costar) and resolved and quantified against standards by high-performance anion-exchange chromatography with pulsed-amperometric detection using a CarboPac PA20 column at 40°C, 50 mM NaOH eluent, and quadruple waveform, as recommended by the instrument manufacturer (Dionex). Glc and Gal coelute under these conditions. Values were normalized against lactose. The insoluble fraction of each sample was tested for starch content with the Total Starch Assay Procedure Kit from Megazyme (amyloglucosidase/α-amylase method) scaled down 10 times. Calculations and statistical analyses were done using Microsoft Excel.

Radiolabeling

For radiolabeling of intact plants, [U-^{14}C]Suc (21.8 GBq mmol^{-1} in 9:1 ethanol:water; MP Biochemicals) was lyophilized to remove the ethanol and concentrate the solution to 1 mM Suc (21.8 MBq mL^{-1}). From this, fresh labeling solution was prepared (0.5 mM [U-^{14}C]Suc, 10 mM MES, pH 5.5, and 1 mM $CaCl_2$) for each experiment. The adaxial, distal tips of the first three adult leaves of intact plants were gently abraded with 220 grit sandpaper, and 2 μL of labeling solution was applied, being careful to keep it localized to the abraded region. Leaves were left for short (1, 3, and 5 min) or long (1, 2, and 4 h) periods under standard laboratory lighting, quickly excised from the plant, placed between two sheets of 3MM paper (Whatman), frozen in powdered dry ice, and lyophilized for 48 h in a chamber held at −30°C. Tissues were then pressed flat between steel plates in a large vice and exposed to Kodak BioMax MR Film for 36 h before developing.

To measure phloem exudation (Turgeon and Medville, 2004), four mature leaves were excised at the stem at 4 h into the light period, weighed, and recut under water, and the petioles were placed on a 24-well microtiter plate with 2 mL of water in each well. *AtSUC2* −/− plants were cut below the cotyledonary node and arranged in 2-mL microfuge tubes cut to 7.5 mm and filled with 200 μL of water. Four replicates (i.e. sibling plants) for each representative line were prepared. The microtiter plates were placed in a plastic chamber with a soaked paper towel to create a high-humidity environment, covered with a sheet of clear plastic, and sealed with an elastic band around the rim of the chamber. The labeling chamber was placed 3 feet below a 400-W metal halide lamp, and the leaves were labeled by mixing 1.11 MBq [^{14}C]$NaHCO_3$ with an excess of 80% lactic acid in the barrel of a 1-mL syringe with a 22-gauge needle extending through the side of the chamber. The 1-mL barrel was then replaced with a 60-mL barrel, and air inside the chamber was circulated by slowly moving the plunger back and forth while keeping the chamber sealed. Labeling was for 20 min, and the metal halide lamp was turned off. The leaf petioles were cut again under the surface of 15 mM EDTA to prevent sealing of the sieve plate pores at the cut surface, and the cut ends were placed in 1 mL of 15 mM EDTA on 24-well microtiter plates. The entire EDTA solution was collected at various time points and replaced with fresh solution. Each sample was mixed with 5 mL of Fisher ScintiSafe Plus 50% (Fisher) liquid scintillation cocktail. After exudation time points were collected, soluble sugars were extracted and a portion of the MCW solution was mixed with 5 mL of liquid scintillation cocktail. The remaining leaf material was cleared with 500 μL of bleach and similarly mixed with 5 mL of liquid scintillation cocktail. Total incorporation was calculated as the sum of the exudates and soluble and insoluble fractions.

ACKNOWLEDGMENTS

We thank Róisín McGarry, Rebecca Dickstein, and Robert Turgeon for critical reading of the manuscript and Karin Devasto for laboratory assistance. We thank two anonymous reviewers for their insightful comments.

Received June 15, 2008; accepted July 17, 2008; published July 23, 2008.

LITERATURE CITED

Aloni B, Wyse RE, Griffith S (1986) Sucrose transport and phloem unloading in stem of *Vicia faba*: possible involvement of a sucrose carrier and osmotic regulation. Plant Physiol **81:** 482–486

Alonso JM, Stepanova AN, Leisse TJ, Kim CJ, Chen H, Shinn P, Stevenson DK, Zimmerman J, Barajas P, Cheuk R, et al (2003) Genome-wide insertional mutagenesis of Arabidopsis. Science **301:** 653–657

Ausubel FM, Brent R, Kingston RE, Moore DD, Seidman JG, Smith JA, Struhl K, editors (2002) Short Protocols in Molecular Biology: A Compendium of Methods from Current Protocols in Molecular Biology, Ed 5. John Wiley & Sons, Hoboken, NJ

Ayre BG, Keller F, Turgeon R (2003) Symplastic continuity between companion cells and the translocation stream: Long-distance transport is controlled by retention and retrieval mechanisms in the phloem. Plant Physiol **131:** 1518–1528

Ayre BG, Kohler U, Turgeon R, Haseloff J (2002) Optimization of transsplicing ribozyme efficiency and specificity by in vivo genetic selection. Nucleic Acids Res **30:** e141

Ayre BG, Turgeon R (2004) Graft transmission of a floral stimulant derived from CONSTANS. Plant Physiol **135:** 2271–2278

Barker L, Kuhn C, Weise A, Schulz A, Gebhardt C, Hirner B, Hellmann H, Schulze W, Ward JM, Frommer WB (2000) SUT2, a putative sucrose sensor in sieve elements. Plant Cell **12:** 1153–1164

Becker D, Kemper E, Schell J, Masterson R (1992) New plant binary vectors with selectable markers located proximal to the left T-DNA border. Plant Mol Biol **20:** 1195–1197

Bornke F, Hajirezaei M, Heineke D, Melzer M, Herbers K, Sonnewald U (2002) High-level production of the non-cariogenic sucrose isomer palatinose in transgenic tobacco plants strongly impairs development. Planta **214:** 356–364

Bush DR (1999) Sugar transporters in plant biology. Curr Opin Plant Biol **2:** 187–191

Carpaneto A, Geiger D, Bamberg E, Sauer N, Fromm J, Hedrich R (2005)

Phloem-localized, proton-coupled sucrose carrier ZmSUT1 mediates sucrose efflux under the control of the sucrose gradient and the proton motive force. J Biol Chem **280:** 21437–21443

Chincinska IA, Liesche J, Krugel U, Michalska J, Geigenberger P, Grimm B, Kuhn C (2008) Sucrose transporter StSUT4 from potato affects flowering, tuberization, and shade avoidance response. Plant Physiol **146:** 515–528

Clough SJ, Bent AF (1998) Floral dip: a simplified method for *Agrobacterium*-mediated transformation of Arabidopsis. Plant J **16:** 735–743

Deeken R, Sanders C, Ache P, Hedrich R (2000) Developmental and light-dependent regulation of a phloem-localised K^+ channel of Arabidopsis. Plant J **23:** 285–290

Giaquinta RT (1976) Evidence for phloem loading from the apoplast: chemical modification of membrane sulfhydryl groups. Plant Physiol **57:** 872–875

Giaquinta RT (1977) Phloem loading of sucrose: pH dependence and selectivity. Plant Physiol **59:** 750–753

Gottwald JR, Krysan PJ, Young JC, Evert RF, Sussman MR (2000) Genetic evidence for the *in planta* role of phloem-specific plasma membrane sucrose transporters. Proc Natl Acad Sci USA **97:** 13979–13984

Grimm E, Jahnke S, Rothe K (1997) Photoassimilate translocation in the petiole of *Cyclamen* and *Primula* is independent of lateral retrieval. J Exp Bot **48:** 1087–1094

Haritatos E, Ayre BG, Turgeon R (2000) Identification of phloem involved in assimilate loading in leaves by the activity of the galactinol synthase promoter. Plant Physiol **123:** 929–937

Haritatos E, Medville R, Turgeon R (2000) Minor vein structure and sugar transport in Arabidopsis. Planta **211:** 105–111

Hayes PM, Patrick JW, Offler CE (1987) The cellular pathway of radial transfer of photosynthates in stems of *Phaseolus vulgaris* L: effects of cellular plasmolysis and para-chloromercuribenzene sulfonic acid. Ann Bot (Lond) **59:** 635–642

Kempers R, Ammerlaan A, van Bel AJE (1998) Symplasmic constriction and ultrastructural features of the sieve element companion cell complex in the transport phloem of apoplasmically and symplasmically phloem-loading species. Plant Physiol **116:** 271–278

Kempers R, van Bel AJE (1997) Symplasmic connections between sieve element and companion cell in the stem phloem of *Vicia faba* L have a molecular exclusion limit of at least 10 kDa. Planta **201:** 195–201

Klepek YS, Geiger D, Stadler R, Klebl F, Landouar-Arsivaud L, Lemoine R, Hedrich R, Sauer N (2005) *Arabidopsis* POLYOL TRANSPORTER5, a new member of the monosaccharide transporter-like superfamily, mediates H^+-symport of numerous substrates, including *myo*-inositol, glycerol, and ribose. Plant Cell **17:** 204–218

Kuhn C, Franceschi VR, Schulz A, Lemoine R, Frommer WB (1997) Macromolecular trafficking indicated by localization and turnover of sucrose transporters in enucleate sieve elements. Science **275:** 1298–1300

Kuhn C, Hajirezaei MR, Fernie AR, Roessner-Tunali U, Czechowski T, Hirner B, Frommer WB (2003) The sucrose transporter StSUT1 localizes to sieve elements in potato tuber phloem and influences tuber physiology and development. Plant Physiol **131:** 102–113

Lacombe B, Pilot G, Michard E, Gaymard F, Sentenac H, Thibaud J-B (2000) A shaker-like K^+ channel with weak rectification is expressed in both source and sink phloem tissues of *Arabidopsis*. Plant Cell **12:** 837–851

Lalonde S, Tegeder M, Throne-Holst M, Frommer WB, Patrick JW (2003) Phloem loading and unloading of sugars and amino acids. Plant Cell Environ **26:** 37–56

Matsukura C, Saitoh T, Hirose T, Ohsugi R, Perata P, Yamaguchi J (2000) Sugar uptake and transport in rice embryo: expression of companion cell-specific sucrose transporter (OsSUT1) induced by sugar and light. Plant Physiol **124:** 85–94

Minchin PEH, Thorpe MR (1987) Measurement of unloading and reloading of photoassimilate within the stem of bean. J Exp Bot **38:** 211–220

Noiraud N, Maurousset L, Lemoine R (2001) Identification of a mannitol transporter, AgMaT1, in celery phloem. Plant Cell **13:** 695–705

Patrick JW (1997) Phloem unloading: sieve element unloading and post-sieve element transport. Annu Rev Plant Physiol Plant Mol Biol **48:** 191–222

Rasband WS (2007) ImageJ. U.S. National Institutes of Health, Bethesda, MD

Reinders A, Schulze W, Kuhn C, Barker L, Schulz A, Ward JM, Frommer WB (2002) Protein-protein interactions between sucrose transporters of different affinities colocalized in the same enucleate sieve element. Plant Cell **14:** 1567–1577

Riesmeier JW, Willmitzer L, Frommer WB (1992) Isolation and characterization of a sucrose carrier cDNA from spinach by functional expression in yeast. EMBO J **11:** 4705–4713

Sambrook J, Russel DW (2001) Molecular Cloning: A Laboratory Manual, Ed 3. Cold Spring Harbor Laboratory Press, Cold Spring Harbor, NY

Sauer N (2007) Molecular physiology of higher plant sucrose transporters. FEBS Lett **581:** 2309–2317

Sauer N, Stolz J (1994) Suc1 and Suc2: Two sucrose transporters from Arabidopsis thaliana; expression and characterization in baker's yeast and identification of the histidine-tagged protein. Plant J **6:** 67–77

Schulz A, Kuhn C, Riesmeier JW, Frommer WR (1998) Ultrastructural effects in potato leaves due to antisense-inhibition of the sucrose transporter indicate an apoplasmic mode of phloem loading. Planta **206:** 533–543

Sivitz AB, Reinders A, Johnson ME, Krentz AD, Grof CPL, Perroux JM, Ward JM (2007) Arabidopsis sucrose transporter AtSUC9: high-affinity transport activity, intragenic control of expression, and early flowering mutant phenotype. Plant Physiol **143:** 188–198

Sivitz AB, Reinders A, Ward JM (2008) Arabidopsis sucrose transporter AtSUC1 is important for pollen germination and sucrose-induced anthocyanin accumulation. Plant Physiol **147:** 92–100

Smith JAC, Milburn JA (1980) Osmoregulation and the control of phloem-sap composition in Ricinus communis L. Planta **148:** 28–34

Truernit E, Sauer N (1995) The promoter of the Arabidopsis *SUC2* sucrose-H^+ symporter gene directs expression of β-glucuronidase to the phloem: evidence for phloem loading and unloading by SUC2. Planta **196:** 564–570

Turgeon R, Ayre BG (2005) Pathways and mechanisms of phloem loading. *In* NM Holbrook, MA Zwieniecki, eds, Vascular Transport in Plants. Elsevier Academic Press, New York, pp 45–67

Turgeon R, Gowan E (1990) Phloem loading in *Coleus blumei* in the absence of carrier-mediated uptake of export sugar from the apoplast. Plant Physiol **94:** 1244–1249

Turgeon R, Medville R (1998) The absence of phloem loading in willow leaves. Proc Natl Acad Sci USA **95:** 12055–12060

Turgeon R, Medville R (2004) Phloem loading: a reevaluation of the relationship between plasmodesmatal frequencies and loading strategies. Plant Physiol **136:** 3795–3803

van Bel AJE (1996) Interaction between sieve element and companion cell and the consequences for photoassimilate distribution: two structural hardware frames with associated physiological software packages in dicotyledons. J Exp Bot **47:** 1129–1140

van Bel AJE (2003) Transport phloem: low profile, high impact. Plant Physiol **131:** 1509–1510

van Bel AJE, Hess PH (2008) Hexoses as phloem transport sugars: the end of a dogma? J Exp Bot **59:** 261–272

Vaughn MW, Harrington GN, Bush DR (2002) Sucrose-mediated transcriptional regulation of sucrose symporter activity in the phloem. Proc Natl Acad Sci USA **99:** 10876–10880

Weigel D, Glazebrook J (2002) Arabidopsis: A Laboratory Manual. Cold Spring Harbor Laboratory Press, Cold Spring Harbor, NY

Wright KM, Roberts AG, Martens HJ, Sauer N, Oparka KJ (2003) Structural and functional vein maturation in developing tobacco leaves in relation to *AtSUC2* promoter activity. Plant Physiol **131:** 1555–1565

Yamada K, Lim J, Dale JM, Chen H, Shinn P, Palm CJ, Southwick AM, Wu HC, Kim C, Nguyen M, et al (2003) Empirical analysis of transcriptional activity in the Arabidopsis genome. Science **302:** 842–846